The geology of the Didymos System. O. S. Barnouin[1], R. L. Ballouz[1], S. Marchi[2], J.-B. Vincent[3], M. Pajola[4], A. Lucchetti[4], R. T. Daly[1], C. M. Ernst[1], E. Palmer [5], R. Gaskell[5], T. Kohout[6], C. Robin[7], N. Murdoch[7], J. Sunshine[8], T. Farnham[8], F. Tusberti[4], J. L. Rizos[8] Y. Zhang[8], F. Ferrari[9], H. Agrusa[8,10], T. Hirabayashi[11], L. Parro[12], S. Cambioni[13], P. Michel[10], S. Ruducan[14], M. Jutzi[14], E. Asphaug[12], M. C. Nolan[12], A. Campo Bagatin[15], J. M. Trigo-Rodriguez[16], A. Zinzi[17], V. Della Corte[18], N. L. Chabot[1], A. S. Rivkin[1], A. F. Cheng[1], E. Dotto[18] and the DART[19] and LICIACube[20] Team, [1]JHUAPL (Laurel, MD, olivier.barnouin@jhuapl.edu), [2]SWRI (Boulder, Co), [3]DLR (Berlin, Germany), [4]INAF (Padua, Italy), [5]PSI (Tucson, Az), [6]U. Helsinki (Helsinki, Finland), [7]ISAE-SUPAERO (Toulouse, France), [8]U. Maryland (College Park, MD), [9]Politecnico di Milano (Milan, Italy), [10]OCA-CNRS (Nice, France), [11]Auburn U. (Auburn, Al), [12]U. Arizona (Tucson, Az), [13]MIT (Cambridge, MA), [14]U. Bern (Bern, Switzerland), [15]U. Alicante (Alicante, Spain), [16]CSIC-IEEC (Barcelona, Catalonia/Spain), [17]ASI (Rome, Italy), [18]INAF (Rome, Italy), [20] https://dart.jhuapl.edu/Team/, [21] https://www.ssdc.asi.it/liciacube/lcc_team.php.

Introduction: The shape and geology of Didymos and Dimorphos are critical to decipher the formation and evolution of the Didymos system. We use images collected by DART's Didymos Reconnaissance and Asteroid Camera for OpNav (DRACO) and LICIACube's color LUKE imager to reconstruct the shapes of both asteroids, and to assess their geology. Taking into account the limitations of the datasets collected, we use the shape of the asteroids, the number of crater candidates present, the size and location of surface boulders, any evidence for surface mass movements, and the presence or lack of surface lineaments on both asteroids to constrain the geological origin and evolution of the Didymos system.

Data employed: DRACO imaged Dimorphos from one orientation, at about 60º phase, with very little change in the emission angle, but was able to collect a small range of emission angles for Dimorphos that allowed for some stereo data. LUKE collected images of both asteroids with phases angles ranging from 60-120º, as LICIACube flew by the south (-Z) hemisphere of both asteroids about ~130 s after DART's impact. The finest-resolution images possessed a ground sample distance of ~3.9 m/pixel for Didymos, and ~0.055 m/pixel for Dimorphos. The global digital terrain models (DTMs) were built using stereophotoclinometry (SPC), which combines both stereo parallax and photoclinometry or surface shading [e.g., 1,2]. Because of the lack of global coverage, the SPC-derived models are further constrained by limb data, and information about the location of the observed terminator. Reflected light from Didymos, as well as the ejecta produced by the DART impact itself reveal the shapes of both asteroids not directly illuminated by the Sun. The well-resolved, illuminated data collected by both DRACO and LUKE covers about 40% of the surface of Didymos, and 23% of the surface of Dimorphos.

Shapes: The extent of Didymos measures (843±5) by (838±15) by (622±5) m but as the shape construction proceeds [3], future changes are expected. The shape resembles a flattened ellipsoid, with some broad concavities, and a subdued and uneven equatorial bulge. The LUKE images above Didymos' south pole show that unlike many other top-shaped asteroids (Bennu being a notable exception [4]), Didymos' equatorial region is not circular, but possesses some angularity.

In contrast, Dimorphos appears very uniform in shape, measuring (177 ± 2) by (174 ± 4) by (116 ± 2) m, matching closely an oblate spheroid [5]. The -Y view of Didymos is well fit by an ellipse except where large boulders protrude; one limb illuminated by Didymos' shine lies below this ellipse.

Geology: Didymos possesses two geological regions. The first region is located at mid-to-low latitudes. It possesses fewer large boulders (>25 m) relative to the higher latitudes, and shows evidence for features that are interpreted to be surface mass movements [6]. The depletion in large boulders and surface concavities gives the mid-latitude a smooth appearance. It may also possess on average a slightly darker albedo [7]. Unlike for Bennu or Ryugu, there are few candidate craters present in the mid-latitudes of Didymos.

The second geological region on Didymos is located at mid-to-high latitudes. This area is more hummocky relative to the first geological region, and possesses a greater number of both large boulders (>25 m) and concavities. The largest boulder is ~68 m in diameter. Some of the concavities are probably large candidate impact craters. The largest of these craters is 205 m in diameter. This is smaller relative to the size of the asteroid than the largest craters seen on most other asteroids.

It is difficult to identify distinct geological units on Dimorphos, although future efforts making use of roughness and albedo data may reveal disparate units [e.g., 8–11]. The surface is dominated by cobbles and boulders ranging from a few 10s of cm to ~16m [12]. Some of the boulders are arranged in campfire-like structures [13]. Others show evidence for rocks on boulders. Some of the boulders appear to be partially buried. Despite the limitations of the viewing geometry, lineaments have been identified across the asteroid;

some of these are associated with smaller cracks seen on rocks. Although efforts are ongoing, evidence for any type of surface motion of Dimorphos boulders has as yet to be reported. Dimorphos does, however possess 15 candidate-craters, based on a careful topographic assessment. These usually possess a depression surrounded by a ring of boulders, consistent with features interpreted as craters on other boulder-rich asteroid surfaces [14–16].

Surface ages: Crater counts suggest that Didymos' age is ~30x older than the surface of Dimorphos. The crater size-frequency distribution (SFD) on Didymos does not follow typical main-belt asteroid production function. This could be because of the poor image quality available, but may also be a result of crater modification from either past surface deformation or recent infilling, as seen at plausible equatorial craters. The main-belt age of Didymos ranges between 15-500Myr depending on the surface strength assumed.

Preliminary Implications: Both Didymos and Dimorphos are likely rubble piles. The extensive evidence for boulders on both objects, a few of which are much bigger than any observable crater could excavate are good indicators of this. The nominal density 2400±300 kg/m3 (~30% porosity [17]) of the system is also consistent with this interpretation, but can also accommodate the possibility for some larger, stronger aggregates. The need for such interior strength is evinced by a none-circular circumference of the asteroid, when viewed from its south pole; it is also necessary to explain the observed surface mass movements. The lack of craters where mass movement are observed indicate recent and plausibly ongoing surface motion.

The flattened shape of Didymos indicates an early episode of re-adjustment due to interior and surface failure that is observed in numerical models of weak rubble pile that fail due to spin-up [e.g., 18-20]. This re-adjustment would have likely modified some of the original crater shapes, leading to possible changes in the observed crater SFD relative to a typical main-belt production function. The re-adjustment could also have rearranged boulders and shards to make the interior stronger [e.g., 21]. After this hypothesized failure event, Didymos likely continued to spin-up leading to the evidence for surface mass movement of a more unconsolidated layer at low to mid-latitudes, and probably ejection of material near the equator.

The age of Dimorphos' surface may constrain the approximate time when Didymos underwent failure, if Dimorphos formed during that failure event. The oblate shape of Dimorphos remains difficult to explain using existing dynamical models. Ellipsoidal proto-Dimorphos seem more likely, given Dimorphos's presumed formation under the tidal influence of Didymos. The fairly uniform, well-mixed nature of Dimorphos' geology also needs to be explained, as well as some ability to support stresses over long distance across the asteroids as evinced by its surface cracks.

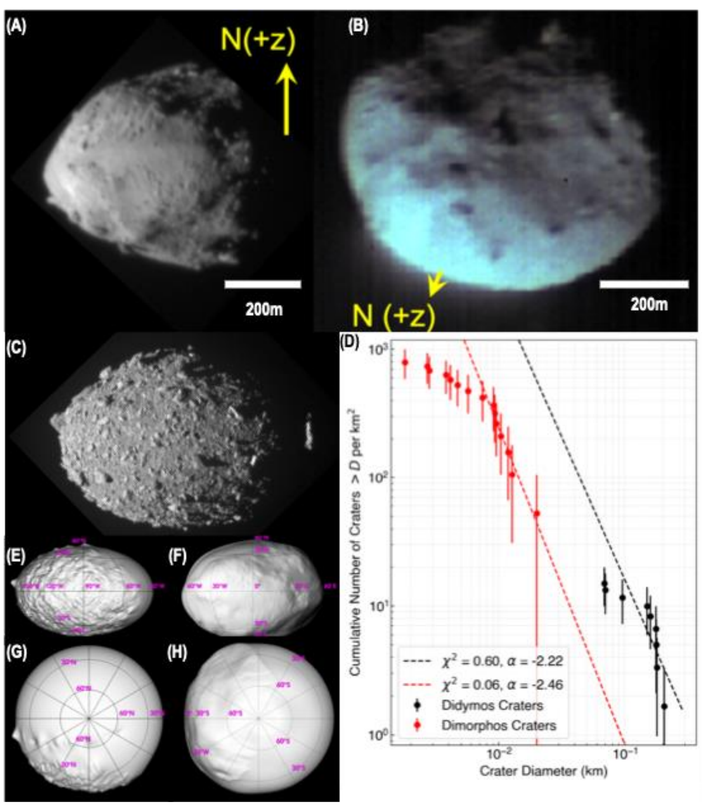

Figure 1. Data used to assess the origin and evolution of the Didymos system: DRACO (a) and LUKE (b) of Didymos; DRACO (c) image of Dimorphos; Crater SFD (D) for both systems; Current shapes of Dimorphos (E,G) and Didymos (F,H).

Acknowledgments: This work was supported by the DART mission, NASA Contract No. 80MSFC20D0004, the Italian Space Agency (ASI) within the LICIACube project (ASI-INAF agreement AC n. 2019-31-HH.0), the FEDER/Ministerio de Ciencia e InnovaciónAgencia Estatal de Investigación research project (PGC2018-097374-B-I00), ESA and CNES.

References: [1] Gaskell, et al. MAPS. 43 (2008) 1049–1061. [2] Daly, et al. Planet. Sci. J. 3 (2022) 207. [3] Palmer et al. LPSC 54 (this issue) [4] Barnouin et al. Nat. Geosci (2019) 12, 247-252. [5] Daly, et al. Nature (in press). [6] Luchetti et al., LPSC 54 (this issue) [7] Sunshine et al. LPSC 54 (this issue) [8] DellaGiustina, et al., Science. 370 (2020). [9] Daly, et al., Science Advances. 6 (2020). [10] Rizos, et al., Icarus. 364 (2021) 114467. [11] Jawin, et al. Icarus. (2022) 114992. [12] Pajola et al. LPSC 54 (this issue) [13] Ballouz, et al., Nature. 587 (2020) 205–209. [14] Hirata, et al. Icarus. 200 (2009) 486–502. [15] Daly, et al., GRL 47 (2020) e2020JE006475. [16] Bierhaus, et al. Nat. Geosci. (2022) 1–7. [17] Cheng et al. 2023 Nature (in press). [18] Sanchez and Scheeres (2012) Icarus 218 (2), 876–894. [19] Zhang et al. (2017) Icarus 294, 98–123 [20] Hirabayashi, et al. (2020), Icarus. 352 (2020) 113946. [21] Roberts et al. (2022) Planetary and Space Science. 204, 105268.